

Communication

TiAl-Based Materials by In Situ Selective Laser Melting of Ti/Al Reactive Composites

Andrey A. Nepapushev ^{1,*}, Dmitry O. Moskovskikh ¹, Ksenia V. Vorotilo ¹ and Alexander S. Rogachev ^{1,2}

¹ Center of Functional Nanoceramics, National University of Science and Technology MISiS, 119049 Moscow, Russia; mos@misis.ru (D.O.M.); m1603570@edu.misis.ru (K.V.V.); rogachev@ism.ac.ru (A.S.R.)

² Merzhanov Institute of Structural Macrokinetics and Materials Science, Russian Academy of Sciences, Chernogolovka, 142432 Moscow region, Russia

* Correspondence: nanoceram_misis_nep@misis.ru; Tel.: +7-495-955-01-13

Received: 16 October 2020; Accepted: 10 November 2020; Published: 11 November 2020



Abstract: Additive manufacturing (AM) of refractory materials requires either a high laser power or the use of various easily melting binders. In this work, we propose an alternative—the use of spherical reactive Ti/Al composite particles, obtained by preliminary high-energy ball milling. These powders were used to produce high-temperature TiAl-based materials during the selective laser melting (SLM) process. When laser heating is applied, mechanically activated composite particles readily react with the release of a considerable amount of heat and transform into corresponding intermetallic compounds. The combustion can be initiated at relatively low temperatures, and the exothermic effect prevents the sharp cooling of as-sintered tracks. This approach allows one to produce dense intermetallic materials with a homogeneous structure in one step via SLM and eliminates the need for powerful lasers, binders, or additional post-processing and heat treatments.

Keywords: titanium aluminides; high-energy ball milling; microstructure; selective laser melting

1. Introduction

Additive manufacturing (AM), also known as 3D printing or selective laser printing, is a rapidly developing technique capable of fabricating a wide range of structures and complex geometries by laser-driven printing of successive layers of materials on top of each other. The process is computer-controlled, and the structure is formed according to the initial CAD (Computer Aided Design) model [1]. This technique enables the fabrication of complex shapes and structures without casting, machining, and subsequent expensive post-processing. These advantages are particularly pertinent for the fabrication of parts with inner cavities and channels [2,3]. The existing AM methods can be roughly divided into 2 subgroups: (1) powder bed fusion; (2) directed energy deposition [4]. In the case of bed fusion, a layer of powder material with a certain thickness is formed on the working table and then selectively treated by a laser, resulting in either sintering or melting of the feedstock powder and formation of the desired structure. In the case of directed energy deposition, no preliminary layers are formed. Instead, the material is fed to a specific location along with the supply of energy. Each technique has characteristic strengths and weaknesses, depending on the specifics of the used processes and materials. Powder bed fusion processes have garnered a lot of traction since they possess the highest accuracy and have a wide range of applications. Among them, the selective laser melting (SLM) process is one of the most widely used techniques, which is applied to a great variety of powdered materials and provides good product quality, reduced processing times, and more reproducible results than laser AM processes which involve binders. Since the feedstock powders are completely melted in the process, SLM enables the production of fully dense components with

a close-to-final shape and mechanical properties equivalent to the bulk materials. SLM can also be applied to manufacturing of light-weight structures (e.g., honeycombs) [5].

Titanium-based alloys and intermetallics are high-performance materials commonly used in various industries. In cases when it is necessary to make complex-shaped or one-of-a-kind workpieces, 3D printing offers great economic benefits by reducing costs and waste. Additionally, the production of titanium aluminides by traditional furnace methods is complicated by the differences in densities, melting and boiling points of titanium and aluminum, as well as by the high affinity of both Ti and Al to oxygen and nitrogen. Therefore, melting and casting of TiAl, as well as 3D printing, must be carried out in a protective atmosphere or vacuum. These issues complicate the additive manufacturing of TiAl-based alloys as well. Since the starting material for SLM is powder, its atomization from pre-cast or fused precursors also requires a protective atmosphere. Additionally, titanium aluminides are quite brittle at room temperature and susceptible to microcracks formed during SLM [6]. Moreover, to melt titanium aluminides, the powders have to be heated to 1400–1500 °C depending on the composition, which requires a powerful laser.

The higher laser power output is associated with higher heating and cooling rates, leading to a reduction in the processing time. However, high energy density is also associated with boiling and splashing of the material in the melt pool, leading to high aluminum losses due to overheating and evaporation [7], as well as increased porosity and a significant deterioration in the surface quality of the final product. The attempts of 3D printing from atomized Ti-Al powders using electron beam melting (EBM) and SLM showed that, along with the aluminum evaporation, prepared materials often suffer from cracks, which are caused by high cooling rates during the process. Another issue is that the obtained materials exhibit metastable and inhomogeneous structures [8]. Given the multiplicity of warmup/cooling down cycles and the formation of heterogeneous structures, additional thermal treatment is required for material homogenization. The problem of material cracking caused by rapid cooling can be partially solved (a) by using preliminary heated substrate plates followed by their slow cooling down and/or (b) by elongating the period of interaction between laser beam and processed material to lower temperature gradients.

In recent years, there has been a growing number of attempts for obtaining various intermetallic compounds by laser processing of reactive powders. This approach allows one to significantly simplify the producing technology of intermetallic compounds by 3D printing. Its advantages include the possibility of obtaining gradient structures and reducing the requirements to the laser power necessary for powder melting since additional heat is released during the process due to the exothermic reaction [9]. In this case, both pre-alloyed powders and a mixture of pure elements can serve as the initial components. To date, this approach was reported for the synthesis of Ti-Al [10,11], Ni-Ti [12,13], and other compounds [14–18].

In this work, we suggest in-situ production of refractory TiAl-based materials by SLM of mechanically formed spherical reactive composite Ti/Al particles. Instead of heating powder particles up to the melting point of TiAl (1450 °C), we are required to pre-heat it only up to the ignition temperature of the exothermal reaction $\text{Ti} + \text{Al} = \text{TiAl}$ ($Q = 75 \text{ kJ/mol}$). The heat generated by the reaction results in increased temperature and conversion of the initial composite particle into intermetallic TiAl particle. An onset temperature of the exothermal reaction for the mixture of elemental Ti and Al powders is about 850 °C, and this temperature decreases down to 640 °C for the same mixture after mechanical activation [19,20]. Utilization of the mechanically activated reactive composite Ti/Al powders with rounded particles allows us to avoid high laser power and overheating of raw powders and sintered items. It is worth noting that SLM of such reactive particles obtained by mechanical treatment in a ball-mill is carried out for the first time.

2. Materials and Methods

High-energy ball milling of Ti-Al mixtures was performed in a planetary ball mill “Activator 2S” (Russia). The rotation velocity for the main planetary disk and the jars was 200 rpm. Parameter

$K = \omega/\Omega$, where ω is the jar velocity and Ω is planetary disk velocity, was equal to 1. The ball-to-powder ratio was 20:1 (360 g of balls/18 g of powders). Ti (LLC “OCHV”, purity 99%, particle size $<45\ \mu\text{m}$) and Al (LLC “OCHV”, purity 98.6%, particle size $<10\ \mu\text{m}$) in stoichiometric ration were treated for 60 min and yielded the rounded Ti/Al powders with a size of 60–100 μm (Figure 1). More details on the high-energy ball milling protocol can be found elsewhere [21]. The as-formed composite powders were used as a feedstock for selective laser printing in SLM 280 HL installation (SLM Solutions Co. Lübeck, Germany). Mechanocomposite powder was spread over an Al substrate as shown in Figure 2 and processed at scan rates (v) of 50, 75, and 100 mm/s in an Ar atmosphere. Due to the limitations related to the low mass of prepared powder ($\sim 200\ \text{g}$), the powder was distributed over the substrate’s surface manually. After passing the beam, a new layer was added. The operation was repeated at least 10 times to produce 1 mm thick plates. The following SLM parameters were used: beam power of 100 W, a spot size of 80 μm , unidirectional scanning strategy without overlapping. The scanning parameters were selected based on literature data [8] taking into account the fact that at a higher laser power the combustion was initiated in the whole powder body instead of the local heating spot (which is undesirable). The manufactured 10 mm \times 5 mm \times 1 mm plates (Figure 2) were then used for structural characterization and mechanical testing.

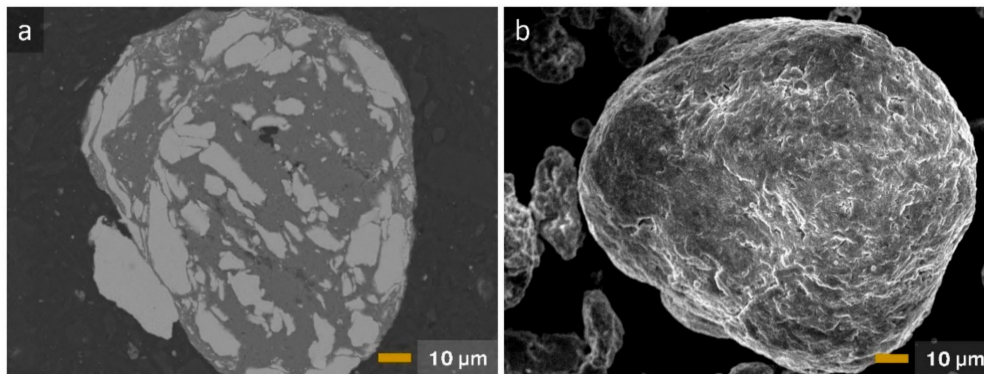


Figure 1. (a) Cross-section and (b) exterior appearance of a nearly spherical particulate of Ti/Al mechanocomposite.

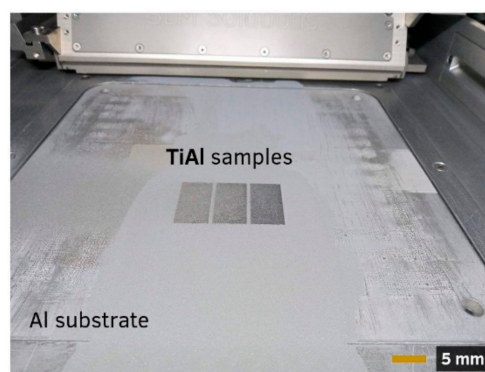


Figure 2. TiAl-based printed plates on the Al substrate.

Synthesized materials were characterized by SEM/EDS using a Jeol JSM7600F microscope (Jeol, Tokyo, Japan) equipped with an EDS accessory INCA SDD 61 X-MAX (Oxford Instruments, Abingdon, UK). Material hardness HV and its elasticity modulus E were determined with a microhardness meter (CSM instruments, Peuseux, Switzerland) under low load (50 mN).

3. Results and Discussion

Figure 3a presents the SEM image of printed material obtained at $v = 50$ mm/s. The material consists of uniaxial TiAl_2 grains 8–12 μm in size with Ti_3Al inclusions (<0.5 μm thick) located on the grain boundaries. The residual porosity does not exceed 0.5%, and the pores were 0.01–0.05 μm in size. The sample obtained at $v = 75$ mm/s (Figure 3b) has a similar structure (uniaxial grains, 5–6 μm in size) but a higher porosity (2%), which can be associated with the higher scan rate. An increase in v to 100 mm/s also led (Figure 3c) to the formation of dense material with a somewhat higher porosity (5%). With increasing v , we observed some decrease in the size of TiAl_2 grains: from 7 μm at 75 mm/s to 3–5 μm at 100 mm/s. Additionally, the needle-like character of Ti_3Al precipitates around the TiAl_2 grains becomes more pronounced.

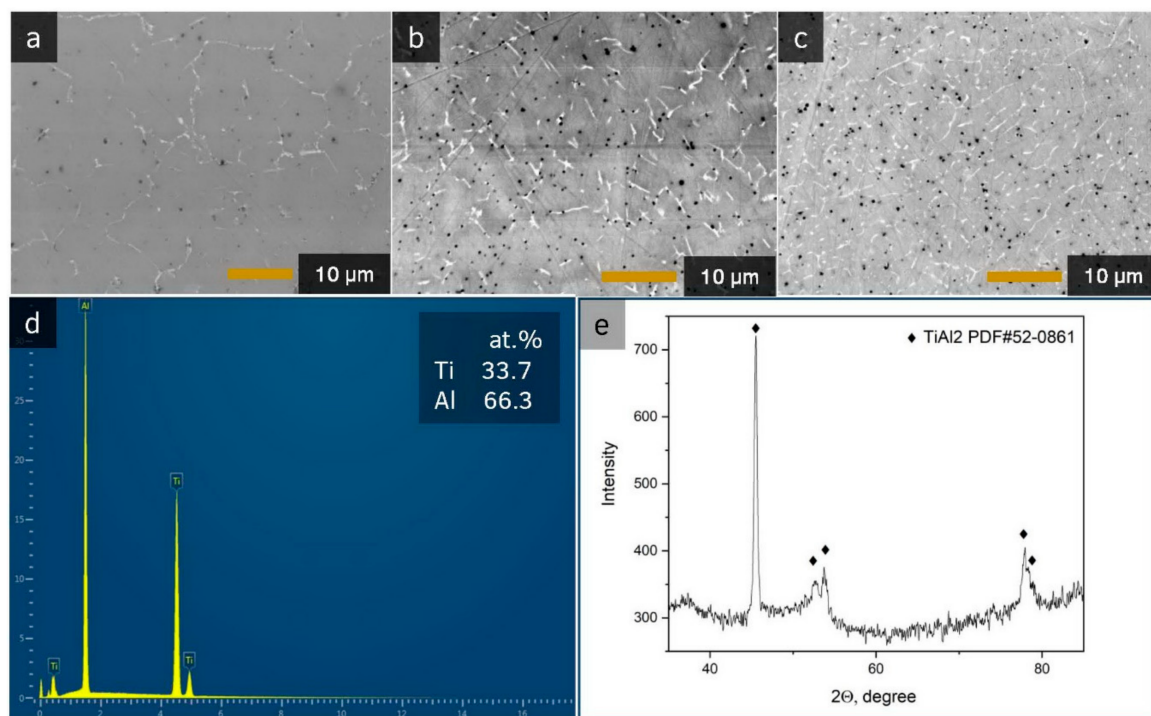


Figure 3. TiAl-based material prepared by selective laser printing at scan rates $v = 50$ (a), 75 (b), and 100 mm/s (c); (d) shows typical elemental composition of printed materials. TiAl_2 grains are shown in grey, Ti_3Al inclusions in bright grey, and pores in black; (e) corresponding XRD analysis.

The EDS results in Figure 3d show that the matrix consists of a TiAl_2 phase, which is confirmed by the XRD investigations (Figure 3e). This is indicative of low Al losses via evaporation. The size of Ti_3Al precipitates is too small to be analyzed by EDS and XRD analysis.

Figure 4 presents the SEM image of the fracture surface in the TiAl-based material prepared at 75 mm/s and reveals the traces of Al melting which accelerates the beam-induced reaction yielding solid solution. It also follows from Figure 4 that the size of product grains (largely equiaxial) is around 3–4 μm while that of pores, 0.5–1.0 μm .

Obtained microstructures are remarkably different from those observed in works that used SLM of pre-alloyed and mixed powders. As mentioned above, non-equilibrium phases are often formed during SLM due to high cooling rates. In [22], TNM-B1 powder (Ti-(42–45) Al-(3–5) Nb-(0.1–2) Mo-(0.1–0.2) B (in at.%) was processed under similar conditions—100 W and 50 mm/s. As a result, a fine-grained lamellar β -microstructure was obtained, which, after annealing at 950 $^{\circ}\text{C}$, transformed into β and α_2 grains with some γ lamellae in α_2/γ colonies. In another work, Gussone et al. investigated the microstructure of the Ti-44.8Al-6Nb-1.0Mo-0.1B alloy after SLM treatment at various laser energy densities [7]. At high energy density, needle-like structures are formed with precipitates of the α_2

phase and β/β_2 grains. Since at this power aluminum readily evaporates and the cooling rate is quite high, a metastable β/β_2 structure is formed. At medium power density, α_2/γ needles are formed, surrounded by γ lamellae and β/β_2 grains. This trend continued at lower energy densities.

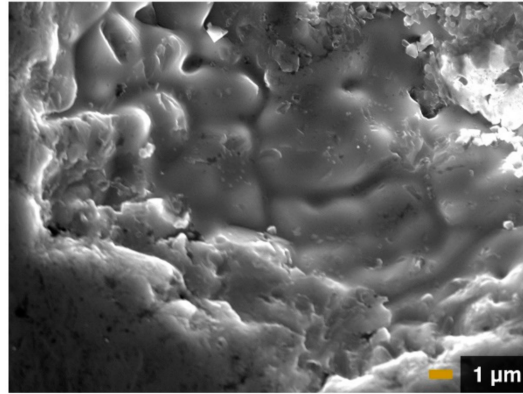


Figure 4. The fracture surface of TiAl materials prepared at a scan rate of 75 mm/s.

Other works related to the SLM of TiAl-based materials, both from pre-alloyed powders [23,24] and from powder mixture [11], show the formation of an inhomogeneous structure, requiring additional temperature post-processing to level the composition. Since we observe a more homogeneous structure in our samples, it can be assumed that in SLM of reactive composites, the mechanism of structure formation differs from that for pre-alloyed powders. The main difference lies in the fact that the phase and structure formation occur over a longer period. After the composite particle reaches the ignition temperature (in our case, the melting point of aluminum), a sharp initiation of the reaction occurs, with a heating rate of 10^3 – 10^5 K/s. At the same time, the reagents are sufficiently fine-grained and are in close contact with each other (Figure 1), which ensures a high rate of chemical interaction. According to the previous investigations [25], TiAl_3 phase forms earlier than others during reaction of titanium with liquid or solid aluminum. It is also known [26] that formation of the TiAl_2 phase (as well as Ti_2Al_5 , $\text{Ti}_5\text{Al}_{11}$ and $\text{Ti}_9\text{Al}_{23}$) occurs through a series of reactions with the obligatory participation of TiAl as one of the initial phases. Correspondingly, we propose the generalized mechanism for the phase formation during SLM of reactive composite particles (Figure 5): (i) formation of the TiAl_3 layer in conditions of aluminum excess on the Ti surface; (ii) continuous interaction of the TiAl_3 layer with Ti and molten Al, which leads to the formation of the TiAl layer; (iii) further reaction of the TiAl and Al with the formation of the TiAl_2 phase. Formation of Ti_3Al precipitates can occur through the reaction between residual titanium and the TiAl_3 phase in the absence of aluminum since it is consumed via interaction with intermediate phases [26] (see Figure 5).

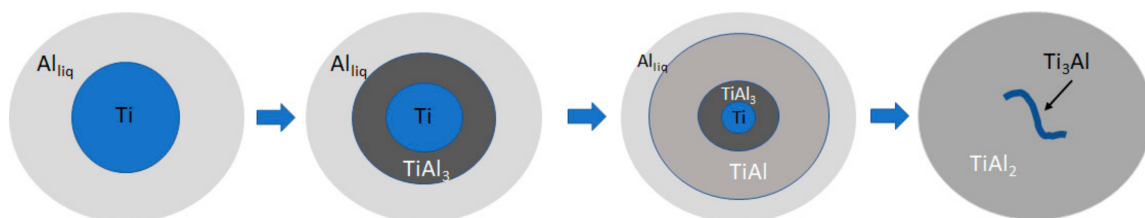


Figure 5. The generalized mechanism for the phase formation during SLM of reactive composite particles.

It is also worth noting that temperature during the phase formation process remains quite high and abrupt cooling does not occur, since, in parallel, reaction is initiated in neighboring particles. The heat generated by the neighboring particles slows down the cooling process, thereby contributing to the formation of a more uniform product structure. Melting of Al promotes the reaction between

compounds and facilitates the sintering process. In this way, our approach alleviates the problems of material patterning and cracking encountered in the processes of 3D printing.

The mechanical properties for the sample printed at the 50 mm/s are shown in Table 1. By micro indentation using the Oliver and Pharr [27] method, we estimated the hardness and elasticity modulus as well as the relative work of plastic deformation (W_p), which characterizes the fracture toughness of the material. The measured values of HV and E on the sample are comparable to or better than those of similar materials [13]. It is also worth noting that as-received samples after SLM usually have higher hardness values than after heat treatment since they have an inhomogeneous structure. In our case, since we have a more uniform structure, it can be expected that a significant decrease in hardness will not occur.

Table 1. Mechanical properties of the sample processed at 50 mm/s scan rate.

Sample	Hardness, H , HV	Work of Plastic Deformation, W_p , %	Young's Modulus, E , GPa
50 mm/s	567 ± 42	80	255 ± 39

4. Conclusions

Our approach allows the synthesis of various materials by in-situ selective laser melting (SLM). Starting powders of nearly spherical reactive mechanocomposite particulates for our process are prepared by high-energy ball milling (HEBM) in a planetary mill. The flowability of such powders is enough for use in a commercial 3D printer. The laser-induced exothermic reaction in reactive particulates yields a required refractory compound in one stage and with no need for binders.

As an example, we have fabricated thin plates of $TiAl_2$ with Ti_3Al inclusions by SLM of Ti/Al mechanocomposite powders. Due to heat release from laser-induced Ti + Al reaction, we managed to avoid the formation of cracks in printed material. Additionally, we have not found any evidence for the evaporation of Al during SLM, because (i) there is no need to heat the as-formed TiAl to its melting point (1456 °C) and (ii) it is sufficient to reach the melting point of Al (660 °C) to initiate the reaction.

Our approach allows us to simplify a process of 3D printing of intermetallic and ceramic items. It opens a route for the fabrication of functionally graded structures and materials and to reduced requirements for laser beam power (due to the contribution of exothermic reactions). In this case, the refractory compounds are formed from starting low-melting reagents. HEBM-produced reactive mechanocomposites are suitable for use in commercially available 3D printers, allowing for a cost-effective alternative for commercially used preliminary alloying of raw powders.

Author Contributions: Conceptualization and writing—review and editing, A.S.R.; production of reactive rounded composites, K.V.V.; SLM experiments, D.O.M.; writing—original draft preparation, A.A.N. All authors have read and agreed to the published version of the manuscript.

Funding: This work was supported by the Russian Ministry for Science and Higher Education in the framework of the Federal Target Program “Research and Development on Priority Directions of the Scientific and Production Complex of Russia for 2014–2020” (agreement no. 14.587.21.0051, project RFMEFI58718X0051).

Conflicts of Interest: The authors declare no conflict of interest.

References

1. DebRoy, T.; Wei, H.L.; Zuback, J.S.; Mukherjee, T.; Elmer, J.W.; Milewski, J.O.; Beese, A.M.; Wilson-Heid, A.; De, A.; Zhang, W. Additive manufacturing of metallic components—Process, structure and properties. *Prog. Mater. Sci.* **2018**, *92*, 112–224. [[CrossRef](#)]
2. Chia, H.N.; Wu, B.M. Recent advances in 3D printing of biomaterials. *J. Biol. Eng.* **2015**, *9*, 4. [[CrossRef](#)]
3. Ngo, T.D.; Kashani, A.; Imbalzano, G.; Nguyen, K.T.Q.; Hui, D. Additive manufacturing (3D printing): A review of materials, methods, applications and challenges. *Compos. Part B Eng.* **2018**, *143*, 172–196. [[CrossRef](#)]
4. Frazier, W.E. Metal Additive Manufacturing: A Review. *J. Mater. Eng. Perform.* **2014**, *23*, 1917–1928. [[CrossRef](#)]

5. Doubenskaia, M.; Domashenkov, A.; Smurov, I.; Petrovskiy, P. Study of Selective Laser Melting of intermetallic TiAl powder using integral analysis. *Int. J. Mach. Tools Manuf.* **2018**, *129*, 1–14. [[CrossRef](#)]
6. Singh, S.; Ramakrishna, S.; Singh, R. Material issues in additive manufacturing: A review. *J. Manuf. Process.* **2017**, *25*, 185–200. [[CrossRef](#)]
7. Gussone, J.; Hagedorn, Y.C.; Gherekhloo, H.; Kasperovich, G.; Merzouk, T.; Hausmann, J. Microstructure of γ -titanium aluminide processed by selected laser melting at elevated temperatures. *Intermetallics* **2015**, *66*, 133–140. [[CrossRef](#)]
8. Chen, W.; Li, Z. Additive manufacturing of titanium aluminides. In *Additive Manufacturing for the Aerospace Industry*; Elsevier: Amsterdam, The Netherlands, 2019; pp. 235–263, ISBN 9780128140635.
9. Gu, D.D.; Meiners, W.; Wissenbach, K.; Poprawe, R. Laser additive manufacturing of metallic components: Materials, processes and mechanisms. *Int. Mater. Rev.* **2012**, *57*, 133–164. [[CrossRef](#)]
10. Grigoriev, A.; Polozov, I.; Sufiiarov, V.; Popovich, A. In-situ synthesis of TiAlNb-based intermetallic alloy by selective laser melting. *J. Alloys Compd.* **2017**, *704*, 434–442. [[CrossRef](#)]
11. Polozov, I.; Sufiiarov, V.; Kantyukov, A.; Popovich, A. Selective Laser Melting of TiAlNb-based intermetallic alloy using elemental powders: Effect of process parameters and post-treatment on microstructure, composition, and properties. *Intermetallics* **2019**, *112*, 106554. [[CrossRef](#)]
12. Wang, C.; Tan, X.P.; Du, Z.; Chandra, S.; Sun, Z.; Lim, C.W.J.; Tor, S.B.; Lim, C.S.; Wong, C.H. Additive manufacturing of NiTi shape memory alloys using pre-mixed powders. *J. Mater. Process. Technol.* **2019**, *271*, 152–161. [[CrossRef](#)]
13. Zhang, B.; Chen, J.; Coddet, C. Microstructure and Transformation Behavior of in-situ Shape Memory Alloys by Selective Laser Melting Ti–Ni Mixed Powder. *J. Mater. Sci. Technol.* **2013**, *29*, 863–867. [[CrossRef](#)]
14. Fischer, M.; Joguet, D.; Robin, G.; Peltier, L.; Laheurte, P. In situ elaboration of a binary Ti-26Nb alloy by selective laser melting of elemental titanium and niobium mixed powders. *Mater. Sci. Eng. C* **2016**, *62*, 852–859. [[CrossRef](#)]
15. Dadbakhsh, S.; Hao, L. Effect of Al alloys on selective laser melting behaviour and microstructure of in situ formed particle reinforced composites. *J. Alloys Compd.* **2012**, *541*, 328–334. [[CrossRef](#)]
16. Zhang, B.; Fenineche, N.-E.; Liao, H.; Coddet, C. Magnetic properties of in-situ synthesized FeNi₃ by selective laser melting Fe-80%Ni powders. *J. Magn. Magn. Mater.* **2013**, *336*, 49–54. [[CrossRef](#)]
17. Minasyan, T.; Aydinyan, S.; Toyserkani, E.; Hussainova, I. In Situ Mo(Si,Al)₂-Based Composite through Selective Laser Melting of a MoSi₂-30 wt.% AlSi10Mg Mixture. *Materials* **2020**, *13*, 3720. [[CrossRef](#)]
18. Gao, C.; Wang, Z.; Xiao, Z.; You, D.; Wong, K.; Akbarzadeh, A.H. Selective laser melting of TiN nanoparticle-reinforced AlSi10Mg composite: Microstructural, interfacial, and mechanical properties. *J. Mater. Process. Technol.* **2020**, *281*, 116618. [[CrossRef](#)]
19. Bizot, Q.; Politano, O.; Nepapushev, A.A.; Vadchenko, S.G.; Rogachev, A.S.; Baras, F. Reactivity of the Ti–Al system: Experimental study and molecular dynamics simulations. *J. Appl. Phys.* **2020**, *127*, 145304. [[CrossRef](#)]
20. Shkodich, N.F.; Kochetov, N.A.; Rogachev, A.S.; Grigoryan, A.E.; Sharafutdinov, M.R.; Tolochko, B.P. Formation of the crystal structure of intermetallic compounds in mechanically activated Ni-Al and Ti-Al systems during self-propagating high-temperature synthesis. *Bull. Russ. Acad. Sci. Phys.* **2007**, *71*, 650–652. [[CrossRef](#)]
21. Nepapushev, A.A.; Moskovskikh, D.O.; Buinevich, V.S.; Vadchenko, S.G.; Rogachev, A.S. Production of Rounded Reactive Composite Ti/Al Powders for Selective Laser Melting by High-Energy Ball Milling. *Metall. Mater. Trans. B* **2019**, *50*, 1241–1247. [[CrossRef](#)]
22. Löber, L.; Schimansky, F.P.; Kühn, U.; Pyczak, F.; Eckert, J. Selective laser melting of a beta-solidifying TNM-B1 titanium aluminide alloy. *J. Mater. Process. Technol.* **2014**, *214*, 1852–1860. [[CrossRef](#)]
23. Li, W.; Liu, J.; Zhou, Y.; Li, S.; Wen, S.; Wei, Q.; Yan, C.; Shi, Y. Effect of laser scanning speed on a Ti-45Al-2Cr-5Nb alloy processed by selective laser melting: Microstructure, phase and mechanical properties. *J. Alloys Compd.* **2016**, *688*, 626–636. [[CrossRef](#)]
24. Li, W.; Liu, J.; Zhou, Y.; Wen, S.; Wei, Q.; Yan, C.; Shi, Y. Effect of substrate preheating on the texture, phase and nanohardness of a Ti-45Al-2Cr-5Nb alloy processed by selective laser melting. *Scr. Mater.* **2016**, *118*, 13–18. [[CrossRef](#)]
25. Školáková, A.; Salvetr, P.; Novák, P.; Vojtěch, D. Formation of Ti-Al Phases during SHS Process. *Acta Phys. Pol. A* **2018**, *134*, 743–747. [[CrossRef](#)]

26. Sujata, M.; Bhargava, S.; Sangal, S. On the formation of $TiAl_3$ during reaction between solid Ti and liquid Al. *J. Mater. Sci. Lett.* **1997**, *16*, 1175–1178. [[CrossRef](#)]
27. Oliver, W.C.; Pharr, G.M. An improved technique for determining hardness and elastic modulus using load and displacement sensing indentation experiments. *J. Mater. Res.* **1992**, *7*, 1564–1583. [[CrossRef](#)]

Publisher's Note: MDPI stays neutral with regard to jurisdictional claims in published maps and institutional affiliations.



© 2020 by the authors. Licensee MDPI, Basel, Switzerland. This article is an open access article distributed under the terms and conditions of the Creative Commons Attribution (CC BY) license (<http://creativecommons.org/licenses/by/4.0/>).